Pentacene Thin Film Growth

Ricardo Ruiz,*,† Devashish Choudhary,‡ Bert Nickel,§ Tullio Toccoli,|| Kee-Chul Chang,† Alex C. Mayer,† Paulette Clancy,‡ Jack M. Blakely,† Randall L. Headrick,⊥ Salvatore Iannotta,|| and George G. Malliaras*,†

Materials Science and Engineering Department and Chemical and Biomolecular Engineering Department, Cornell University, Ithaca, New York 14853-1501, Department für Physik and CeNS, Ludwig-Maximilians-Universität, München, Germany, IFN Istituto di Fotonica e Nanotecnologie Sezione di Trento CNR-ITC, Povo Trento, Italy, and Department of Physics, The University of Vermont, Burlington, Vermont 05405

Received March 15, 2004. Revised Manuscript Received September 9, 2004

Pentacene stands out as a model molecule among organic semiconductors due to its ability to form well-ordered films that show a high field effect mobility. We discuss the processes involved in pentacene film growth, emphasizing differences with respect to inorganic films. The influence of growth parameters such as the substrate nature and temperature, the deposition rate, and the kinetic energy of the molecular beam on the structure and morphology of pentacene films are discussed. Finally, we overview recent attempts to model pentacene film nucleation and growth, and draw attention to the role of dislocations.

1. Overview

Organic thin films with high structural order are required to implement the novel electronic and optical applications that have been proposed for devices based on small conjugated molecules. Among the candidates for technologies such as large area[1,2] and mechanically flexible organic electronics,[3,4,5] pentacene stands out for its relatively high field effect mobility[6,7] and its ability to form ordered films[8,9] on various types of substrates, making it one of the best candidates for organic thin film transistors (OTFTs). Enormous progress in improving the field effect mobility of OTFTs has been made in the last fifteen years.[1,10] It is also well-known that the charge transport properties of conjugated molecules like pentacene are intrinsically correlated with their crystalline structure, with the degree of orientation, and with grain size, although the exact form of these correlations is not yet well understood. Hence, controlling and optimizing film quality is essential to achieve the device applications sought for pentacene.

Pentacene ($C_{22}H_{14}$) is a planar molecule composed of five benzene rings linked as shown in Figure 1. In its bulk phase, pentacene has a triclinic structure (space group $P\bar{1}$) and a density of 1.32 g/cm^3. There are two molecules per unit cell arranged in a herringbone configuration.[11] Pentacene is reported to have two polymorphs in its bulk phase.[12−15] Vacuum-deposited thin films, however, differ from the bulk, forming a structure that has been referred to as the "thin film phase".[16] The bulk polymorph shown in Figure 1[12] has been found to coexist with the "thin film phase" on evaporated thin films beyond a certain critical thickness.[17] Since charge transport properties in pentacene depend on an efficient π-orbital overlap between the molecules, it is important to understand the structure and molecular packing in pentacene thin films as well as the growth mechanisms that produce such structures.

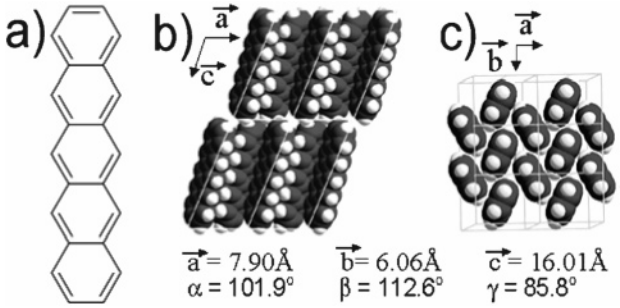

Figure 1. (a) Chemical structure and (b−c) bulk crystalline structure of pentacene.

The van der Waals nature of the intermolecular bonding and the anisotropy of the individual molecules are responsible for the main differences in the growth mechanisms between organic and inorganic thin films. These differences bring a new world of opportunities for technology applications but also bring new challenges in understanding the fundamental properties of thin films of organic molecular crystals. To model and control organic thin film growth from the vapor phase, it is necessary to adapt the conventional models for inorganic molecular beam epitaxy so that these major differences are incorporated.

A considerable amount of work on film morphology, degree of order, crystal quality, and nucleation and growth processes in pentacene thin films has been carried out recently. The present paper is a review of

* Authors to whom correspondence should be addressed. G.G.M. Tel: 607-255-1956. Fax: 607-255-2365. E-mail: george@ccmr.cornell.edu. R.R. Tel.: 607-255-0705. E-mail: rr253@cornell.edu.
† Materials Science and Engineering, Cornell University.
‡ Chemical and Biomolecular Engineering, Cornell University.
§ Ludwig-Maximilians-Universität.
|| IFN Istituto di Fotonica e Nanotecnologie Sezione di Trento CNR-ITC.
⊥ The University of Vermont.

10.1021/cm049563q CCC: $27.50
Published on Web 10/16/2004

advances in understanding pentacene thin film growth. We first give, in section 2, a summary of the main processes involved in thin film growth from the vapor phase with emphasis on the differences between organics and inorganics, as well as a list of the most common techniques available to probe thin film growth. Section 3 reviews the influence of growth parameters such as substrate material, substrate temperature, deposition rate, and the kinetic energy of the molecular beam on pentacene film growth. Section 4 discusses some applications of growth models to explain recent experiments on the nucleation and growth of pentacene thin films as well as the impact of dislocations. Though of great importance, we do not attempt here to describe the electronic properties of pentacene films. In the interest of brevity, the review will not cover thin film growth of materials other than pentacene. Reviews and comparisons of other organic thin films can be found elsewhere.[18−20] For the same reason, the paper will not include deposition of pentacene from solution.[21,22] Finally, the paper will focus only on thin film technology and thus it will not cover the growth of pentacene single crystals.[23]

2. Introduction To Growth Processes and Growth Kinetics

2.1 Organic vs Inorganic Film Growth. Inorganic thin film growth by molecular beam epitaxy (MBE) and organic growth by molecular beam deposition (OMBD) have some similarities and some fundamental differences. In MBE, the substrate is a clean single crystal and the adsorbates are usually single atoms or dimers that chemisorb on the surface. Moreover, the atoms are assumed to have an isotropic shape (sphere) so that the orientation of the adatom relative to the substrate or to other atoms is irrelevant for the strength of the interaction. Inorganic crystal growth relies on the rather strong covalent or ionic bonds of the adsorbates to the substrate. For the same reason lattice matching is usually a requisite for crystal growth, because it avoids stress buildup.

In general, thin films grow in one of the three modes depicted in Figure 2a: layer-by-layer (Frank−van der Merwe mode), layer-plus-island (Stranski−Krastanov mode), and island mode (Volmer−Weber). In the inorganic case,[24] the layer-by-layer mode occurs when the atoms diffuse to form two-dimensional (2D) islands and are more strongly bonded to the substrate than to other adatoms. The island mode occurs when the interactions within the adsorbates are stronger than to the substrate, forming three-dimensional (3D) islands. The layer-plus-island mode occurs whenever the layer formation becomes less favorable and the film develops islands after one or more layers as a means to lower its free energy.

In the case of organic molecular crystals such as pentacene, the interactions between molecules in the crystal are rather weak van der Waals interactions.[11,25] Furthermore, since the molecules are not spherically symmetric, the strength of the molecule−molecule and molecule−substrate interactions (and so the free energy of the system) depends on the relative orientation of the ad-molecules. Thus, the conditions for a given growth mode will depend on a delicate balance of the anisotropic

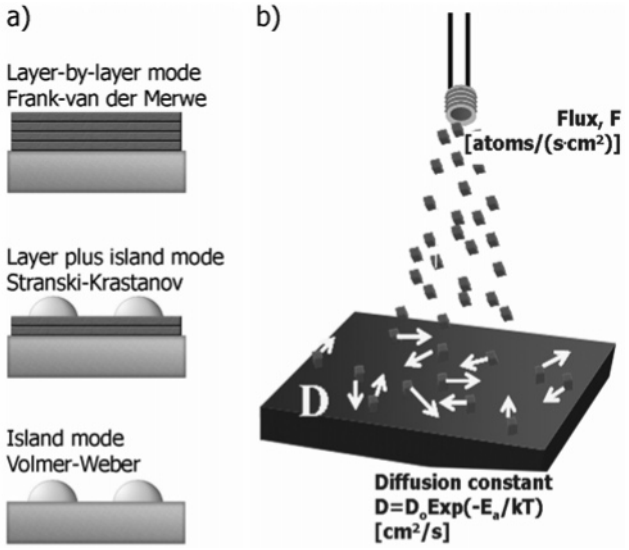

Figure 2. (a) Growth modes: layer-by-layer, layer-plus-island, and island mode. Inorganic layer-by-layer occurs when the adsorbate−substrate interactions are stronger than the adsorbate−adsorbate interactions. For organic molecules, the condition may be reversed for certain inert substrates. (b) Atomistic representation of the nucleation and growth of a film grown by MBE.

interactions between the molecules, their neighbors, and the substrate.[26] For example, if the substrate is inert and flat, molecules such as pentacene have a tendency to self-assemble forming crystalline domains[9,27] regardless of the crystallographic orientation of the substrate. The molecules stand nearly vertical and a layer-by-layer growth occurs when the lateral pentacene−pentacene interactions are more important than either the pentacene−substrate or pentacene−pentacene interlayer ones.[28−31] This opens up new possibilities for multilayer structures since lattice matching is no longer a requirement.[32]

Despite the differences with inorganic films, there are some similarities that can be exploited to understand the physical processes in organic thin film growth. Some cases of coincident epitaxy[18] (sometimes referred to as van der Waals epitaxy[33] or quasi-epitaxy[34]) on organic films have been reported. For pentacene, in particular, diffusion-limited aggregation[28] and scaling theories[35−37] have been applied to understand the formation of the first layer on inert surfaces, and a distributed growth model[38] has been employed for subsequent layers. The formation of an epitaxial layer of pentacene on Cu[39] and commensurate layers on Ag substrates[40] have also been reported.

2.2 Nucleation and Growth. Deposition of thin films by OMBD starts by evaporating the organic material from a Knudsen cell as illustrated in Figure 2b. The molecular beam is aimed at the substrate at a flux or rate of F molecules per unit area per unit time. The incoming molecules adsorb onto the substrate and then diffuse with a diffusion constant, D. The adsorbates then can do one of the following:[24] re-evaporate into vacuum, nucleate 2D or 3D islands, aggregate onto existing islands, get captured at a step or defect sites, or diffuse into the substrate. In the case of the formation of the first layer of pentacene on an inert, flat substrate, the last two processes can be neglected. There is no

diffusion into the substrate and, as shown in Figure 3, there is no preferential nucleation on stepped surfaces.[41]

The nucleation and formation of the first layer can be understood and modeled from atomistic theories starting with the kinetic rate equations[42]

$$\frac{dN_1}{dt} = F - \frac{N_1}{\tau_a} - 2U_1 - \sum_{j=2}^{\infty} U_j$$

$$\frac{dN_j}{dt} = U_{j-1} - U_j; (j \geq 2) \qquad (1.1)$$

where N_1 and N_j are the concentrations per unit area of molecules (for the case of OMBD) and clusters of size j, respectively. U_j values are the capture rates of molecules by clusters of size j, and τ_a is the mean re-evaporation time. Several ways to simplify the rate equations have been proposed[24] depending on the particular system to be modeled. Some assumptions include the formation of 3D clusters[43] or 2D clusters[44] or the occurrence of coarsening effects.[45] Others have to take into account that the probability of capture is larger for fractal islands than for compact islands according to the relationship between the island cross section and its mass.[44,46] This is particularly important for pentacene since it has been observed to grow in fractal shape.[28] The particular solutions of the rate equations will lead to characteristic island size distributions and scaling relationships[43,44] that help identify and characterize the evolution of the first layer.

For systems where desorption can be neglected ($\tau_a \rightarrow \infty$), as in the case of pentacene deposited on substrates close to or below room temperature, the kinetics of the surface diffusion process[47] is determined by the ratio of D to F ($R = D/F$). System-specific properties such as the nucleation density, N, and the average island size, $A(\theta)$, are determined by R through[44]

$$N = CR^{-\chi} \approx \frac{\theta}{A(\theta)} \qquad (1.2)$$

where θ is the layer coverage and the exponent χ is related to the critical island size,[48] i, by $\chi = i/(i + 2)$. Islands comprising $i + 1$ molecules (or adatoms in the case of inorganics) are stable against dissociation.[24]

Applications of these concepts and models of film growth to pentacene are possible. However, to have a full understanding of the physics involved in the formation of the layers, the models have to include the anisotropy of the molecule, the weak pentacene−pentacene van der Waals interactions and the pentacene−substrate interactions for either inert or reactive substrates as will be discussed in Sections 3.1 and 3.2.

2.3 Relevant Growth Parameters. Since $R = D/F$ governs the dynamics of film growth, three experimental parameters can be used to tune film morphology. These three parameters are the substrate material, substrate temperature, and deposition rate. The substrate material modifies the diffusion pre-factor, D_0 and the diffusion energy barrier, E_a, and will also determine the orientation of the molecules with respect to the surface. The substrate temperature, T, determines the kinetic energy of the adsorbates to overcome the diffusion barrier ($D = D_0\text{Exp}[-E_a/kT]$) and the deposition rate, F, determines the density of molecules diffusing on the substrate per unit area per unit time. Understanding the effects of these three experimental parameters is crucial to engineer high-quality thin films for organic electronic devices.

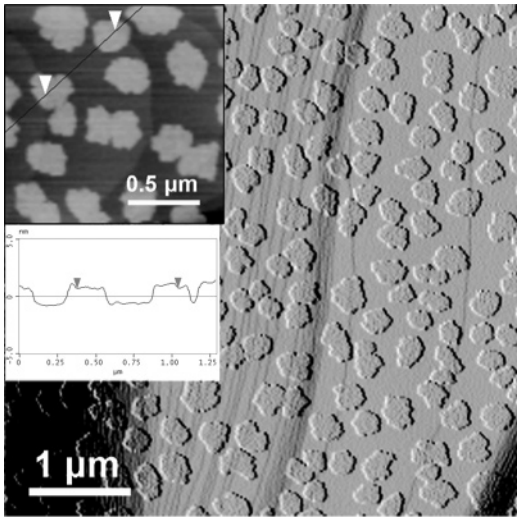

Figure 3. AFM micrograph (amplitude signal) of submonolayer pentacene film on Si steps showing there is no preferential nucleation on the steps.[41] The stepped Si surface was oxidized with native silicon oxide prior to pentacene deposition. Inset: height signal showing that islands nucleated on regions with steps follow the step morphology. The cross-section shows that the Si steps are reproduced on the pentacene islands (arrows).

2.4 Common Techniques to Probe Film Structure and Growth Dynamics. The vast majority of experimental surface science methods developed to characterize the structure and electronic properties of deposited films can, in principle, be applied to the case of pentacene.[49] The low conductivity of this molecular solid and its sensitivity to electron beam damage introduce some restrictions but already a large number of studies of growth structures and corresponding electronic properties have been successfully carried out.

Direct or real space imaging methods include scanning electron microscopy (SEM),[16,50] and photoelectron emission microscopy (PEEM).[28,36] Scanning tunneling microscopy (STM) has been employed to identify the orientation of pentacene molecules on semiconducting[51,52] and metallic[29,40,53] crystals. The atomic force microscope (AFM) is probably the most widely applied method for postdeposition characterization of film morphology[17,30,54] and can be an excellent tool for detecting small scale surface features. Scanning Kelvin probe microscopy has provided useful information on the grain/domain boundaries and electrode interfaces that have an important effect on the transport properties of continuous films.[55,56]

Monitoring of diffracted beams (X-ray diffraction, XRD[16,17,27,30,54,57], electron diffraction,[9,27] or low-energy He diffraction[58]) during pentacene growth yields information on the growth mode, the degree of order, and domain arrangement of the polycrystalline film, as well as the development of surface roughness. XRD is particularly powerful as it can be used to monitor in real time the formation of the first layer[35] and the development of thicker films[30,38] as well as to extract information on the crystalline quality of the films.[17,59]

Along with these crystalline structure techniques a broad range of methods is available for probing the accompanying electronic structure development. X-ray and ultraviolet photoelectron spectroscopy (XPS and UPS) can be used to follow the development of the filled states during growth and to measure their location relative to the vacuum level[60−62] while Penning ionization electron spectroscopy can be used to determine the spatial electron distributions of the outermost layer in a film.[63] Optical techniques applied to pentacene films include second harmonic generation[64] and Raman spectroscopy.[65]

3. Influence of Growth Parameters on Pentacene Film Growth

3.1 Nature of the Substrate. In general, the orientation of the pentacene molecules with respect to the substrate (especially for the first monolayer) is determined by the balance between the pentacene−substrate and pentacene−pentacene interactions.[28,29,31] In the present section, experimental evidence of the influence of the substrate in the formation of the first layer and the subsequent film morphology for various substrate materials will be discussed followed by ab initio calculations for pentacene−substrate interactions.

When pentacene is deposited onto flat, inert substrates such as some of the oxide or polymeric dielectrics, pentacene molecules stand nearly vertical on the substrate.[1,9,16,17,27,31] It is believed that the (001) plane has the lowest surface energy in pentacene crystals.[31,66] With a weakly interacting substrate where intralayer pentacene−pentacene interactions are stronger than pentacene−substrate interactions, pentacene will tend to form crystals with the (001) plane parallel to the substrate plane, that is, leaving the lowest energy surface exposed.

On the other hand, if the substrate is a more reactive one, like clean Si[28,51,52] or a clean metal,[67−70] the interactions with the substrate become more important and may involve charge transfer at the interface. This makes pentacene molecules lie flat on the surface.

The morphology and the orientation of pentacene films has been studied on a variety of substrates and some typical morphologies are reproduced in Figure 4a-d.[28,68,71−73]

Among the inert substrates, perhaps the most common one is SiO_2[9,16,17,28,30,35,38,54,74,75] (Figure 4a) because of its application as a gate dielectric for transistors. But there are also other potential gate-dielectric materials that have been employed as substrates for pentacene growth such as SiN,[54,76] or Al_20_3.[77] Polymeric substrates (Figure 4b) include, but are not limited to, polymethyl methacrylate (PMMA),[78,79] poly(3,4-ethylenedioxythiophene)/poly(styrenesulfonate) (PEDOT/PSS),[61] polyvinylphenol (PVP),[3] collodion,[27] and polyester,[27] while high-k dielectrics include BZT,[80] BST,[81] and BaTiO.[82] X-ray diffraction data (available for almost all the above substrates except the high-k dielectrics) shows that on inert films, pentacene molecules stand with their long molecular axis nearly perpendicular to the substrate. However, the inter-planar spacing (d_{001} = 15.4 Å)[16] is different from that in pentacene bulk crystals (d_{001} = 14.5 Å).[12] The structure obtained in the evaporated thin films has been referred to in the literature as the "thin film phase".[16] Recent grazing incidence X-ray diffraction (GID) data from a single layer of pentacene grown on silicon oxide estimate the unit cell vectors[83] a = 7.578 Å, b = 5.909 Å, and γ = 89.95°. Other recent GID from submonolayer and multilayer films[84] obtained a rectangular lattice with unit vectors a = 7.6 Å, b = 5.9 Å,- and γ = 90°. This structure was reported to be independent of film thickness (up to 190 Å) and substrate temperature (within the range from 0 to 45 °C). Before the "thin film phase" was identified as different from the bulk, electron diffraction experiments of pentacene on collodion[27] estimated a = 7.41 and b = 5.76 Å. However, a triclinic structure was reported recently on salt substrates,[85] and another orthorhombic cell with four molecules in the unit cell was also reported[86] (although in that structure molecules were not standing vertical on the substrate).

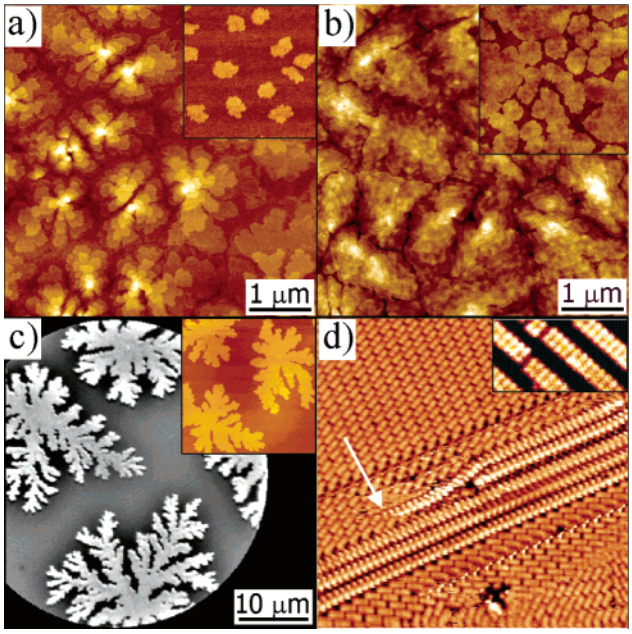

Figure 4. Morphologies of pentacene films on various substrates. (a) 3ML nominal deposition on SiO_2. Inset: submonolayer islands.[71] (b) Pentacene on PEDOT:PSS.[72] Inset: submonolayer islands on PMMA.[71] On both polymeric substrates pentacene domains form layered grains with single-molecule steps while mimicking the substrate roughness. (c) Submonolayer islands of pentacene on Si (after a layer of pentacene lying flat on the substrate) [Reprinted with permission from ref 28. Copyright 2001 Nature Publishing Group.]. Inset: pentacene on H-terminated Si.[71] (d) STM images of Pentacene on Ag. The arrow indicates the next pair of molecules tilting up from the planar position [Reprinted with permission from ref 68. Copyright 2003 Elsevier]. Inset: STM image of pentacene on Cu showing the molecules lying flat on the substrate in an ordered manner [Reprinted with permission from ref 73. Copyright 2002 by the American Physical Society].

A special case of inert substrates are those treated with self-assembled monolayers (SAMs). SiO_2 is often treated with SAMs prior to pentacene deposition to improve the field effect mobility[87,88] or to control the surface carrier density[89] in OTFTs. Growth mechanisms on those treated substrates are less detailed in the literature but we can point out a few differences. On SiO_2 substrates, conventional cleaning procedures such as wet chemistry or UV-ozone treatment leave a highly hydrophilic surface on which water adsorbs.[30] On the other hand, SAMs change the wetting properties of SiO_2

creating a hydrophobic surface[90] (surface roughness usually increases as well). The role of the ad-layer of water during film growth on SiO_2 is not well understood yet. Pentacene grain sizes on SAMs are usually smaller than those on SiO_2[50] (probably due to the increased roughness), although structurally, pentacene deposited on octadecyltrichlorosilane (OTS) seems to have a lower dislocation density (0.5×10^{11} cm^{-2}) than pentacene on SiO_2 (0.9×10^{11} cm^{-2}) for the same growth conditions.[59] However, both, bulk and thin film phases are commonly found within films deposited on OTS.[50,59] Al_2O_3 substrates have also been treated with a variety of SAMs[7] showing layer-by-layer growth for the first two layers of pentacene on 1-phosphonohexadecane.

Pentacene on passivated Si substrates also grows with the long axis nearly perpendicular to the substrate.[28,30] Silicon dangling bonds can be passivated with hydrogen atoms[30] or with SAMs such as cyclohexene.[28] If Si is not passivated before pentacene deposition, then the first monolayer of pentacene molecules chemisorbs[51,52,91] on the substrate forming a monolayer of lying-flat molecules, but subsequent layers grow with the molecules standing nearly perpendicular to the substrate[28] (Figure 4c).

On metals, the interactions between pentacene and substrate are stronger than the pentacene−pentacene interactions and the first layer grows with the long molecular axis parallel to the surface (Figure 4d). These strong interactions lead to the formation of a large interface dipole that may increase hole injection barriers.[61,62] STM studies reveal that pentacene can grow in a commensurate manner on different crystalline metal surfaces. On Ag,[40] Au,[60,92] and Cu,[73] submonolayer films consist of rows of pentacene molecules that can be aligned head-to-head[68] or side-by-side.[67,73] In the case of Cu(110),[73] it has been suggested that the periodicity of the rows is dictated by the formation of surface charge density waves as pentacene is adsorbed onto the substrate. Beyond the first monolayer, molecules can continue stacking on top of each other for a few layers[29] or they can rearrange by tilting their short axis,[68] or they can have a configuration different from that of the first layer.[39,58] Other metals that have been used as substrates for pentacene in the literature are Ca,[93] Pt,[94,95] Sm,[96,97] Pd,[55] Ni,[55] and stainless steel.[98]

The shape of the molecule and the pentacene−substrate interactions for the different possible orientations were recently taken into account in a computation of the chemical bonding interactions of a pentacene molecule on a Si (100)−(2×1) surface.[99] The most stable adsorption sites perpendicular and parallel to the dimer rods (shown in Figure 5) were found to have binding energies per molecule of 5.02 and 4.92 eV, respectively. These strong interactions agree with experimental observations that thermal desorption fails to completely remove the chemisorbed layer on Si (the molecule may, indeed, decompose into fragments[100]). The calculated structures also suggest that the first monolayer of pentacene adsorbed on the silicon substrate is highly strained and serves as the template for nucleating subsequent layers.

Passivation of the silicon (100) surface with SAMs completely changes the nature of the interactions between the pentacene molecules and the substrate

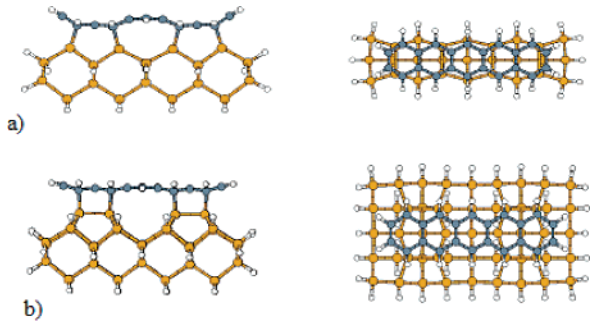

Figure 5. Equilibrium structures of the most favored pentacene adsorption sites on the Si (100) surface calculated using tight-binding. (a) Adsorption site parallel to the dimer row, binding energy 4.92 eV. (b) Adsorption site perpendicular to the dimer row, binding energy 5.02 eV.

from a strongly chemically bonded condition to one dictated by weak van der Waals interactions. Using a Gaussian computational algorithm to simulate the interactions between a pentacene molecule and a cyclopentene-passivated substrate revealed very weak interaction energies of 0.4 and 0.08 eV per molecule when the long molecular axis is parallel or perpendicular to the substrate, respectively.[101] The stronger interactions in the parallel orientation result from the larger number of hydrogen atoms that are able to interact with the π cloud of the pentacene molecule. Calculations of the interaction energies of a pentacene molecule with a β-quartz silica substrate revealed similarly weak interactions in the parallel and perpendicular orientations (0.22 and 0.17 eV, respectively). These values are comparable to interaction energies extrapolated from thin film growth studies on inert substrates.[31]

3.2 Substrate Temperature and Deposition Rate. Following eq 1.2, it is clear that increasing the substrate temperature and lowering the deposition rates will decrease the nucleation density and therefore increase the average grain size. Indeed, there exists a considerable amount of data to support this prediction.[9,35,50,54] However, when trying to adjust growth parameters to customize film morphology, there are other issues that need to be considered such as temperature-activated competing processes that result in nucleation of the bulk phase, surface diffusion limits, dislocation or defect formation, and favorable thermodynamic conditions for layered growth.

The "thin film phase" of crystalline domains in pentacene thin films is a substrate-induced structure different from the bulk.[16] It has been reported that nucleation of the bulk phase starts beyond a certain critical film thickness,[17,54] d_c. The value of d_c has also been reported to decrease with increasing substrate temperature.[17,64] Typical values of d_c for films grown at room temperature are around 100−150 nm[17,64,76] and can go down to ~30 nm for films grown at ~90 °C.[17] The influence of the deposition rate on d_c and on the nucleation of the bulk phase is less studied, although there is one report[54] that suggests that d_c is independent of F. Therefore, from a practical point of view, the nucleation of the bulk phase sets an upper limit for the substrate temperature when looking for single-phase films.

On the other hand, too low a substrate temperature or too large a deposition rate may limit surface diffusion

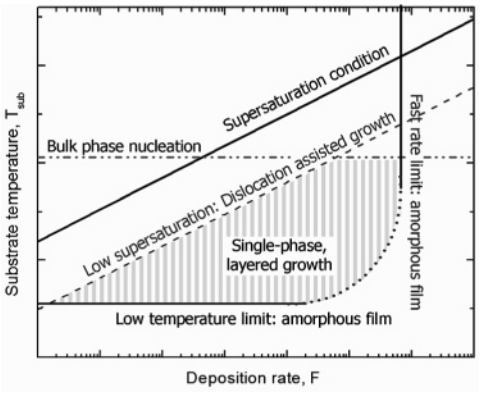

Figure 6. Qualitative description of the limits for layer-by-layer pentacene growth. A crystal can be grown below the line for the supersaturation condition. The high-temperature limit is set by the nucleation of the bulk phase. Amorphous films result at high rates or low substrate temperatures. At low supersaturations, growth may become dislocation-assisted.

of the adsorbates producing an amorphous film. X-ray diffraction experiments revealed that growth at $T_{sub} = -196$ °C ($F = 0.5$ Å/s) results in an amorphous film.[16,102] In general, even if some out-of-plane ordering can be achieved, films grown below 0 °C show high nucleation densities[35] and poor film quality.[64] This would set a lower limit for T_{sub}. There is also one report on an amorphous film grown at an extremely fast rate by flash evaporation,[74] confirming that high rates could also prevent the formation of ordered films.

Lowering the deposition rate and/or increasing T_{sub} brings the system to low supersaturations where dislocation-assisted growth[103] plays a larger role. Layer-by-layer growth requires the nucleation of new islands every time a layer is completed. There is an energy barrier associated with the aggregation of the critical number of molecules required to form a stable cluster.[24] At low supersaturation, the nucleation rate is very low and growth can occur predominantly at existing surface steps associated with screw dislocations.

Finally, layer-by-layer growth can only occur if the necessary thermodynamic conditions are met.[24] Thermodynamically, crystal growth is an irreversible process and occurs when the chemical potential of the vapor, μ_v, exceeds that of the growing deposit, μ_s. Because of finite island size effects and interactions with the substrate, the chemical potential difference necessary to promote growth may be significantly different from the value needed to create the homogeneous bulk phase. If we denote by $\Delta\mu$ the difference between chemical potential of the vapor and that of the homogeneous solid under the specified growth conditions [$\Delta\mu = \mu_v - \mu_s$], growth of 2D islands on a dissimilar substrate material can occur even when $\Delta\mu < 0$.[31]

In summary, increasing the substrate temperature or lowering the deposition rate to improve the grain size has to be done with caution as it can result in island-mode growth or no growth at all below supersaturation, or it can favor the nucleation of the bulk phase or the formation of dislocations. All these restrictions set the limits for 2D growth (ideal for device applications[1,104]). These ideas are pictured qualitatively in Figure 6.

On the basis of what has been presented so far, it is important to distinguish between the first layer and subsequent layers. Nucleating and growing a layer of pentacene on SiO_2 or on another substrate is different from growth on a layer of pentacene. Pentacene−substrate interactions are different and therefore the surface diffusion constant will be different so that nucleation densities and grain sizes may be different in the second layer than in the first layer. On SiO_2 substrates, for example, the nucleation density is higher for the first layer than for the second layer.[30] As a consequence, second layer islands grow on top of more than one first-layer domain. Given that the first layer-islands are randomly oriented with respect to each other, the larger second-layer islands will, in part, be misoriented with some regions of the first layer and this may induce strain. However, the effects of this strain have not yet been studied.

As mentioned in section 2, the final orientation of the first layer depends on the balance between the pentacene−substrate and the pentacene−pentacene interactions. To predict the most favorable orientation of the molecules with respect to the substrate it is necessary to take into account all possible orientations. Submonolayer growth of an anisotropic molecule on a variety of substrates has been modeled recently using a lattice-based kinetic Monte Carlo (KMC) simulation.[101] Consideration of two competing rate processes, deposition rate (or flux, F) and surface diffusion (a function of temperature, T_{sub}) within this KMC framework provides the ability to map out a landscape of possible thin film morphologies. Figure 7 shows morphology maps for three different pentacene−substrate scenarios: (a) stronger interactions in a parallel (red) orientation as compared to the perpendicular (blue) orientation, (b) interactions in both orientations are comparable, and (c) stronger interactions in the perpendicular configuration. Even slight changes in the relative interactions between the substrate and molecule have a dramatic effect on the morphology of the thin films. For example, higher temperatures and lower deposition rates result in compact islands with a high percentage of molecular alignment. The critical nucleus size, defined by the smallest cluster to evolve into a stable island was found to range from 6 to 16 molecules. This is in reasonable agreement with experimental data for thin film growth on SiO_2 and cyclohexene passivated Si surfaces where its value has been estimated to be around four[35] and six[36] respectively. The mode of diffusion of the organic molecules was found to involve molecules diffusing across the substrate in an orientation parallel to the substrate and subsequently aggregating. An intriguing synergetic "flipping" of molecules into an upright position was observed once a critical nucleus has been formed. Once again, incorporating the anisotropy of the interactions of the molecule into the physical models yields a better understanding of differences between organic and inorganic thin film growth and gives a spectrum of the possible morphologies, some of which have already been observed experimentally.

3.3 Kinetic Energy of the Pentacene Molecular Beam. The role played by the initial energy state of molecular precursors in the growth of organic films is often overlooked, mainly because it usually cannot be controlled in conventional growth methods. For example, in OMBD the oven temperature controls both the average energy of the subliming molecules (in a

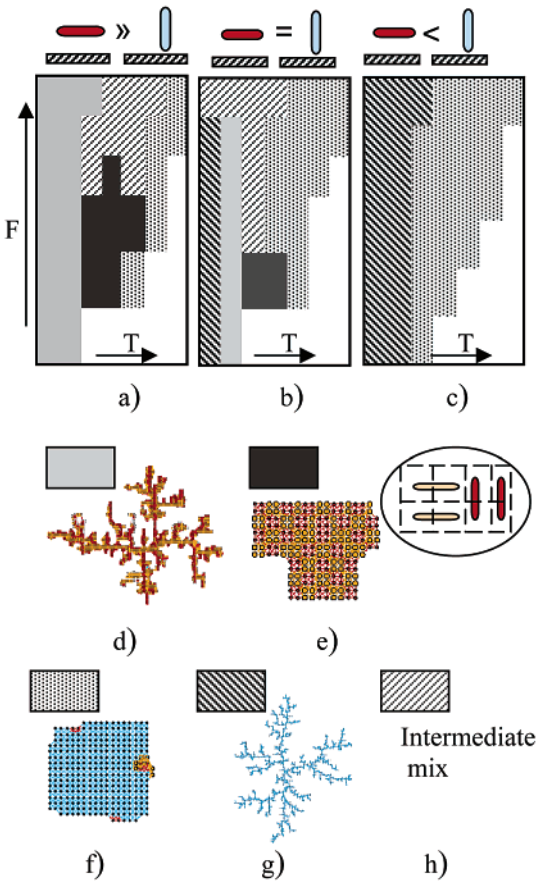

Figure 7. Morphology diagram of pentacene molecules on various substrates calculated using a KMC simulation along with the color-codes for the various morphologies observed in the figures. Here *F* is the rate of the deposited molecules and *T* is the temperature of the substrates. (a) Morphology diagram when molecule−substrate interaction in parallel (red) orientations exceed those for upright (blue) orientations. (b) Morphology diagram when molecule−substrate interactions in both orientations are similar. (c) Morphology diagram when molecule−substrate interaction in an upright orientation is greater than the molecule−substrate interaction in a parallel orientation. (d) All molecules parallel to the substrate in a dendritic arrangement. (e) Compact formation with all molecules parallel to the substrate. (f) Compact structure with majority of the molecules in perpendicular orientation. (g) Dendritic structure with majority of molecules in perpendicular orientation. (h) Transition structures which could not be classified as belonging to any distinct group.

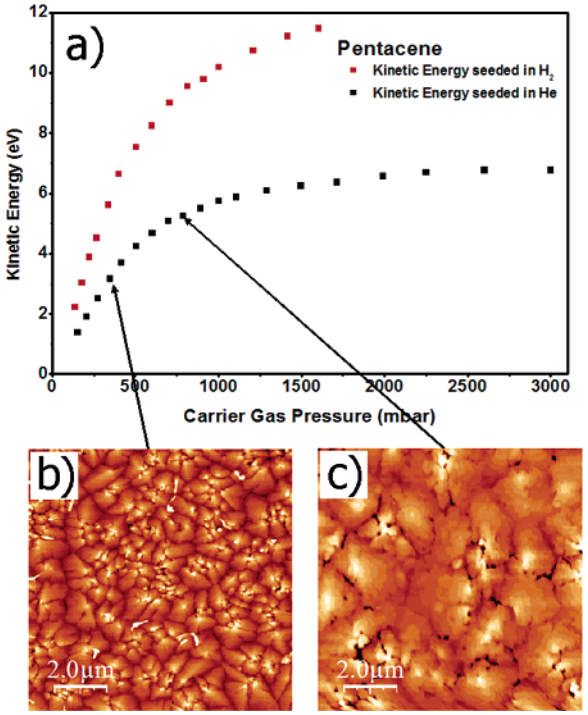

Figure 8. (a) Kinetic energy as a function of the pressure of the carrier gas at a constant source temperature of 210 °C. The carrier gas pressure is directly proportional to the dilution. (b) Tapping mode-AFM micrograph of a 100 nm thick film grown with a kinetic energy of 3.5 eV. (c) Tapping mode-AFM micrograph of a 100 nm thick film grown with a kinetic energy of 5.5 eV.

narrow range of thermal energies) and the deposition flux. On the other hand, molecule−surface interaction dynamics and reactivity are known to strongly depend on the initial kinetic and rotational−vibrational states of the molecule. As previously discussed, in OMBD the implicit assumption is that thermalization with the surface is the mechanism dominating the process so that the temperature of the substrate and the flux rate are considered the major parameters controlling the growth for a given substrate. In a series of experiments,[105] the group of Trento has been studying the growth of organic films on different substrates showing that hyperthermal energies give unprecedented control on the growth,[106] reactivity[107] morphology, and structure[108] of molecular thin films. This has been achieved using supersonic beam methods[109] and seeding the sublimed molecular vapors into a much higher density of lighter carrier gases such as He and H_2. The method allows preparation of well collimated, highly directional beams of organic molecules controlling their kinetic energy from a fraction of eV to several tens of eV by changing the dilution rate (or seeding). An example is shown in Figure 8a, where the kinetic energy of pentacene as a function of the seeding in He and H_2 is plotted for a source operated at about 210 °C. The whole energy range up to 12 eV could be easily covered. This is a quite interesting range where several surface processes can be activated ranging from physisorption to chemisorption to reactivity. It should be noted that a fast and effective cooling, down to a few K, of the rotational−vibrational degrees of freedom can also be induced producing also a preferential alignment of the molecular backbone along the beam axis.[110] SuMBE growth of pentacene has been explored on different substrates demonstrating interesting features. On the atomically clean (111) surface of Ag, thermal effusive beams give rise to amorphous films, confirming the reported frustration in achieving ordering of pentacene on this surface:[73] on this same substrate other organic molecules grow in quite nicely ordered structures at least up to a few monolayers.[111] A much better result was achieved by using a He seeded beam of pentacene at a kinetic energy of about 5 eV: highly ordered thin films were grown at a substrate temperature of 200 K.[58] This study, including atomic and X-ray diffraction, has shown that the first wetting layer has a crystalline structure with the molecules lying flat on the surface, while from the second layer up to about the 50th layer, a different ordered structure is formed having in-plane lattice parameters matching the bulk crystalline phase. At

lower kinetic energies, already at about 0.4 eV, the ordering of such a structure results to be strongly depleted, demonstrating the key role that the initial energy of the molecules plays in the growth. The process can be schematically assimilated to a sort of local annealing caused by the rearrangement of the energy during the collision with the surface. Also, the morphology of much thicker films is affected as shown by AFM observations. Thermal beams on room-temperature substrates give rise to typically unstructured amorphous films constituted by round ovoidal grains on the scale of hundreds of nm.[105] Only when the kinetic energy is over a few eV can one achieve a typical polycrystalline structure with the morphology shown in Figure 8b where the AFM micrograph of a film, about 100 nm thick grown on SiO_2, is shown. The crystallites (typically 1 μm wide) are characterized by a lamellar growth, the terraces of which have the height of a molecule standing with its backbone upward with respect to the surface. The effect of the kinetic energy can be pushed even further, by increasing the kinetic energy over about 5 eV. Here the crystallites are much larger (see Figure 8c) with wider terraces producing a more homogeneous film with a rms corrugation of 6.5 nm over the 10 μm $\times$ 10 μm (vs 7.5 nm of the 3.5 eV grown film).

The overall picture that emerges from the data is that the initial kinetic energy can really be exploited to control structure and morphology of thin film on different substrates and different thicknesses from the monolayer up to hundreds on nm. This makes very appealing a more widespread use of supersonic-MBE growth.

4. Application of Growth Models To Pentacene Thin Film Nucleation and Growth

4.1 First Layer Formation of Pentacene on Inert Substrates: Dynamic Scaling Theory and Other Atomistic Theories. When deposited on inert substrates, such as silicon oxide[30,36] or passivated Si,[28,82] pentacene molecules diffuse on the substrate nucleating monolayer islands with fractal shapes[28] that resemble those of diffusion-limited aggregation.[112] This characteristic signature served as a motivation to apply conventional concepts of diffusion-mediated growth to the formation of the first pentacene layer on silicon oxide.[35] Diffusion-mediated growth involves four qualitatively different steps.[24,44] Initially, molecules diffuse on an almost bare substrate and when a critical number of them meet a stable nucleus is formed. In a second (intermediate) step, adsorbates still nucleate new islands but also start aggregating into existing ones. Later, in the aggregation regime, the incoming material aggregates into the existing islands only. Finally, islands coalesce. In the aggregation regime there is no nucleation of new islands leading to scaling relations for the island size distribution and island separation at different coverages.

An example of two different submonolayer coverages in the aggregation regime of pentacene on silicon oxide are shown in the inset of Figure 9a. Visual inspection shows that island size and separation are quite regular. A detailed analysis of the island size distribution for different coverages is shown in Figure 9a. With increasing coverage, the average island size increases and the distribution broadens. All data points collapse on a universal curve, if the proper scaling is applied[35,44] (Figure 9b). It is possible to model the distribution of the universal scaling curve[48] (solid line in Figure 9b) according to the critical cluster size, i. The least-squares fit implies $i = 3$, i.e., once 4 pentacene molecules join, this nucleus will grow rather than decay. The dynamic scaling confirmed that the formation of the first layer is a diffusion-mediated process and that former diffusion models can be applied to the first monolayer of pentacene on SiO_2.

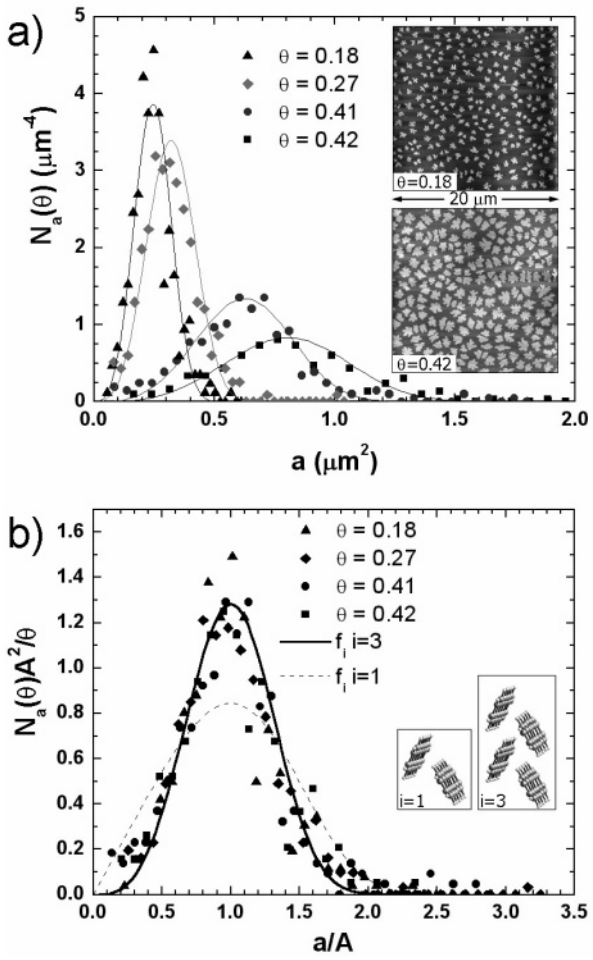

Figure 9. (a) Island size distribution $N_a(\theta)$ of pentacene islands at various coverages. Inset: AFM micrographs of pentacene islands at 0.18 and 0.42 ML. (b) Scaled island size distribution. The scaling function $f(u)$ for a critical cluster size of ($i = 3$) is indicated by the solid curve. Reprinted with permission from ref 35. Copyright 2003 American Physical Society.

4.2 Distributed Growth Model. Modeling of thicker films is much more complex as many parameters come into play when the molecules adsorb on different layers. Synchrotron X-ray scattering, however, provides a powerful technique to probe film growth in real time from the early stages of film formation. In the kinematical approximation,[113] the X-ray intensity for specular reflection by a thin film is given by

$$I = |r_{sub}e^{-i\phi} + r_{film}\sum_n \theta_n e^{-iqdn}|^2 \qquad (1.3)$$

where r_{sub} is the reflection amplitude of the substrate, r_{film} is the amplitude from a layer of the film, θ_n is the coverage of the nth layer of the film, q is the momentum

transfer, d is the interlayer spacing in the film (assuming d is constant for all coverages), and ϕ is the phase difference between the waves reflected by the substrate and the first layer of the film. In the anti-Bragg configuration, q is chosen such that $q \cdot d = \pi$, which corresponds to the $(00^1/_2)$ reflection. In this configuration, the scattered intensity from a pentacene layer will cancel the intensity from the layer directly below. The destructive interference leads to increased sensitivity and has been used in the past to study real-time growth of inorganic[114] and organic[115,116] films.

By means of eq 1.3, X-ray scattering provides a way to test models that predict the evolution of coverage, $\theta_n(t)$, as a function of time for each layer. A simplified way to approach the problem in a first approximation is by employing a distributed growth model[117] which consists of a simplification of the rate equations. In this model, molecules arrive at the film at an effective deposition rate v_{eff} (which accounts for possible desorption) and incorporate onto it. Molecules that land on top of the nth layer (where the 0th layer is the bare substrate), may diffuse and incorporate on the step edge of the $n + 1$ layer, or transfer down to the top of the $n - 1$ layer to be incorporated into the nth layer. Thermal desorption of molecules as well as transfer to adsorption sites on top of the $n + 1$ layer are neglected. The former is a good assumption for a substrate held at room temperature, while the latter is usually the case if there is an asymmetrical Erlich−Schwoebel barrier.[118] Accordingly, the rate of change for the coverage, θ_n, of the nth layer is then given by[117]

$$\frac{d\theta_n}{dt} = \nu_{\text{eff}}(\theta_{n-1} - \theta_n) - \alpha_{n-1}\nu_{\text{eff}}(\theta_{n-1} - \theta_n) + \alpha_n\nu_{\text{eff}}(\theta_n - \theta_{n+1}) \quad (1.4)$$

Eq 1.4 states that of the $\nu_{\text{eff}}(\theta_{n-1} - \theta_n)$ adsorbates landing on top of the $n - 1$ layer per unit time, a fraction α_{n-1} transfers down to the $n - 1$ layer while a fraction $(1 - \alpha_{n-1})$ remains on top of the $n - 1$ layer to be incorporated into the step edges of the nth layer. Similarly, the third term in eq 1.4 accounts for the fraction α_n that transfers down from layer $n + 1$ to the nth layer.

Detailed information on the expression for the coefficients α_n can be found in the literature.[38] Here we focus only on the solutions for θ_n for pentacene films deposited on silicon oxide at room temperature and at a deposition rate of 4 Å/min. Figure 10a shows the anti-Bragg X-ray intensity as a function of the total amount of pentacene deposited. The intensity oscillations are an indication of a layer-by-layer type of growth for the first few monolayers. The solid line is a least-squares fit of the distributed model (eq 1.4) to the X-ray data. In Figure 10b, the fractional coverage for each layer (the solutions for θ_n) is plotted as a function of total thickness.

Even though the simple distributed model does not account for possible lattice variations[119] or include mechanisms other than surface diffusion, it was found to reproduce the essential features of the X-ray data and give an adequate description of the evolution of the coverage for the early stages of growth.

However, as the total coverage increased, the intensity oscillations damped out and disappeared after the 6th layer, indicating that layer-by-layer growth stopped, giving rise to a rough film. When compared to AFM images, the surface was found to be rougher than predicted by the distributed growth model, suggesting that not only surface diffusion, but other mechanisms such as dislocation-assisted growth, may be playing a role.

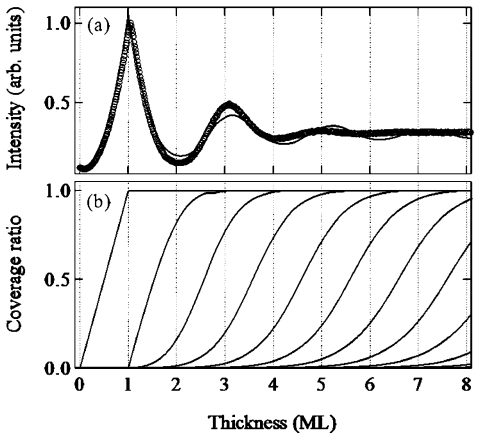

Figure 10. (a) Anti-Bragg oscillations during pentacene growth. The line is a fit to the distributed model. (b) Coverage of each layer vs total coverage. Reprinted with permission from ref 38. Copyright 2004 Elsevier.

4.3 Effects of Dislocations. As mentioned before, layer-by-layer growth imposes an energy barrier to nucleate new islands every time a layer is completed. Therefore, initial layer-by-layer growth tends to convert into a much faster, defect-assisted growth mode. The presence of a screw dislocation in the crystal provides a spiral step on which admolecules aggregate continuously at modest supersaturations.[49]

In the simplest scenario, a single screw dislocation promotes growth in a spiral pattern. Sometimes it is more probable to find pairs or even groups of dislocations.[120] It is also possible that a hollow core[59] forms, in which case the surface energy of the empty core balances the buildup of strain energy (being concentrated in the core of the screw dislocation). Two neighboring screw dislocations can have in general equal or opposite signs (that is, both can turn clockwise or counterclockwise, or one of each). Figure 11 displays a phase signal AFM micrograph of a double screw dislocation of opposite sign on the center of a pentacene grain.

Screw dislocations are accompanied by edge dislocations to adjust the different splaying branches. Since dislocations disturb the crystalline order, it is possible to determine dislocation densities from the analysis of Bragg and diffuse scattering intensities. Dislocations induce a nonthermal Debye−Waller damping of the Bragg intensities (Figure 12a), as well as an additional diffuse scattering around the (resolution limited) delta-shaped Bragg component (Figure 12b and c).

From a detailed analysis,[59] straight dislocation densities of 2.1, 0.9, and 0.5 $10^{11}/\text{cm}^2$ were extracted for deposition on H-terminated Si, oxidized Si, and OTS terminated Si, respectively. Dislocation densities in pentacene thin films are quite high, with films deposited on OTS resulting in the lowest dislocation density.

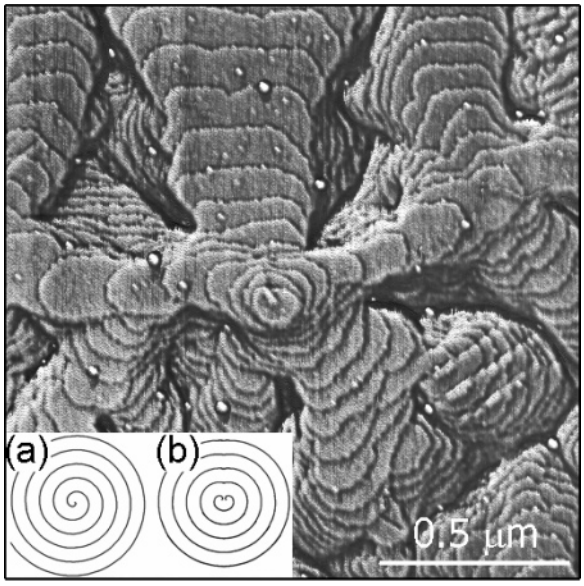

Figure 11. AFM micrograph showing the phase signal on a pentacene grain. The image shows the double screw dislocation of opposite sign on the center of the grain. The inset is a cartoon representation of (a) a single and (b) a double screw dislocation of opposite sign.

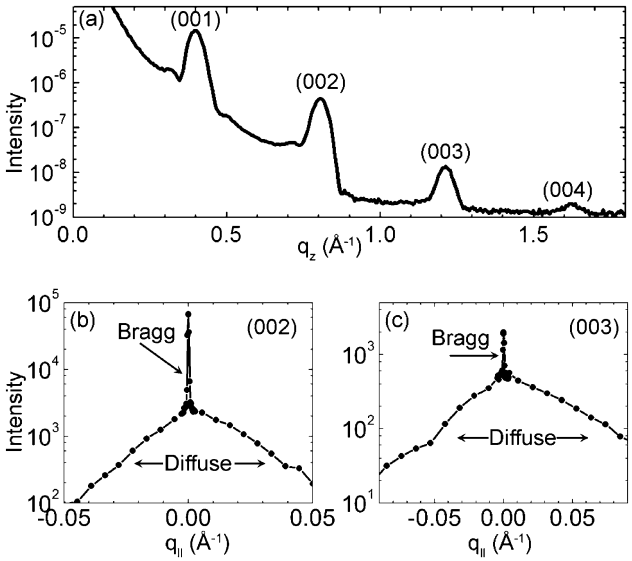

Figure 12. X-ray diffraction from an 8 ML pentacene thin film deposited on H-terminated Si. (a) X-ray reflectivity shows a series of Bragg peaks of the (00L) type. (b−c) Rocking scans around the (00L) Bragg peaks exhibit a sharp Bragg component and additional diffuse scattering.

5. Conclusions

In conclusion, we have reviewed recent experimental and theoretical work exploring the influence of growth parameters on the structure and morphology of vacuum-deposited pentacene films, as well as recent models of pentacene film nucleation and growth. Weak intermolecular bonding and highly anisotropic intermolecular interactions lead to interesting growth physics. When the pentacene−pentacene interactions are stronger than the pentacene−substrate ones, the first monolayer grows with the long molecular axis nearly perpendicular to the substrate. Strong interactions with the substrate, observed in metals and clean silicon, force the molecules to lie with the long axis parallel to the substrate. A diffusion-mediated model has been applied to understand the formation of the first layer on inert substrates, and a distributed model has been applied to describe the formation of thicker films. Taking into account the identifying characteristics of organic molecules (weak intermolecular bonding and highly anisotropic interactions) is crucial to understanding and controlling pentacene film growth.

Acknowledgment. This work was supported with grants from the CCMR, a Materials Research Science and Engineering Center of the National Science Foundation (DMR-9632275), from the Naval Research Laboratory (N00173-00-1-G003), and from the Department of Energy (DEFG0203ER46032).

References

(1) Dimitrakopoulos, C. D.; Malenfant, P. R. L. *Adv. Mater.* **2002**, *14* (2), 99.
(2) Knipp, D.; Street, R. A.; Krusor, B.; Apte, R.; Ho, J. *J. Non-Cryst. Solids* **2002**, *299−302* (2), 1042.
(3) Klauk, H.; Halik, M.; Zschieschang, U.; Eder, F.; Schmid, G.; Dehm, C. *Appl. Phys. Lett.* **2003**, *82* (23), 4175.
(4) Zschieschang, U.; Klauk, H.; Halik, M.; Schmid, G.; Dehm, C. *Adv. Mater.* **2003**, *15* (14), 1147.
(5) Sheraw, C. D.; Zhou, L.; Huang, J.-R.; Gundlach, D. J.; Jackson, T. N.; Kane, M. G.; Hill, I. G.; Hammond, M. S.; Campi, J.; Greening, B. K. *Appl. Phys. Lett.* **2002**, *80* (6), 1088.
(6) Lin, Y.-Y.; Gundlach, D. J.; Nelson, S. F.; Jackson, T. N.*IEEE Electron Device Lett.* **1997**, *18* (12), 606.
(7) Kelley, T. W.; Boardman, L. D.; Dunbar, T. D.; Muyres, D. V.; Pellerite, M. J.; Smith, T. Y. P. *J. Phys. Chem. B* **2003**, *107* (24), 5877.
(8) Minakata, T.; Nagoya, I.; Ozaki, M. *J. Appl. Phys.* **1991**, *69* (10), 7354.
(9) Laquindanum, J. G.; Katz, H. E.; Lovinger, A. J.; Dodabalapur, A. *Chem. Mater.* **1996**, *8* (11), 2542.
(10) Horowitz, G. *Adv. Mater.* **1998**, *10* (5), 365.
(11) Silinsh, E. A. *Organic Molecular Crystals. Their Electronic States.* Springer-Verlag: Berlin, 1980.
(12) Campbell, R. B.; Robertson, J. M.; Trotter, J. *Acta Crystallogr.* **1962**, *15* (3), 289.
(13) Holmes, D.; Kumaraswamy, S.; Matzger, A. J.; Vollhardt, K. P. C. *Chem. -- Eur. J.* **1999**, *5* (11), 3399.
(14) Mattheus, C. C.; Dros, A. B.; Baas, J.; Meetsma, A.; de Boer, J. L.; Palstra, T. T. M.*Acta Crystallogr. Sect. C: Cryst. Struct. Commun.* **2001**, *57*, 939.
(15) Della Valle, R. G.; Venuti, E.; Brillante, A.; Girlando, A. *J. Chem. Phys.* **2003**, *118* (2), 807.
(16) Dimitrakopoulos, C. D.; Brown, A. R.; Pomp, A. *J. Appl. Phys.* **1996**, *80* (4), 2501.
(17) Bouchoms, I. P. M.; Schoonveld, W. A.; Vrijmoeth, J.; Klapwijk, T. M. *Synth. Met.* **1999**, *104* (3), 175.
(18) Hooks, D. E.; Fritz, T.; Ward, M. D. *Adv. Mater.* **2001**, *13* (4), 227.
(19) Schreiber, F. *Phys. Status Solidi A* **2004**, *201* (6), 1037.
(20) Witte, G.; Woll, C. *J. Mater. Res.* **2004**, *19* (7), 1889.
(21) Afzali, A.; Dimitrakopoulos, C. D.; Breen, T. L *J. Am. Chem. Soc.* **2002**, *124* (30), 8812.
(22) Brown, A. R.; Jarrett, C. P.; deLeeuw, D. M.; Matters, M. *Synth. Met.* **1997**, *88* (1), 37.
(23) Karl, N. Growth of single crystals. In *Organic Electronic Materials: Conjugated Polymers and Low Molecular Weight Organic Solids*; Farchioni, R., Grosso, G.; Springer: Berlin, 2001; pp 222−225.
(24) Venables, J. A.; Spiller, G. D. T.; Hanbucken, M. *Rep.n Prog. Phys.* **1984**, *47* (4), 399.
(25) Karl, N. *Synth. Met.* **2003**, *133−134*, 649.
(26) Last, J. A.; Hillier, A. C.; Hooks, D. E.; Maxson, J. B.; Ward, M. D. *Chem. Mater.* **1998**, *10* (1), 422.
(27) Minakata, T.; Imani, H.; Ozaki, M.; Saco, K. *J. Appl. Phys.* **1992**, *72* (11), 5220.
(28) Meyer Zu Heringdorf, F.-J.; Reuter, M. C.; Tromp, R. M. *Nature* **2001**, *412*, 517.
(29) Kang, J. H.; Zhu, X. Y. *Appl. Phys. Lett.* **2003**, *82* (19), 3248.
(30) Ruiz, R.; Nickel, B.; Koch, N.; Feldman, L. C.; Haglund, R. F.; Kahn, A.; Scoles, G., Pentacene ultrathin film formation on reduced and oxidized Si surfaces. *Phys. Rev. B: Condens. Matter Mater. Phys.* **2003**, *67* (12), 125406.

(31) Verlaak, S.; Steudel, S.; Heremans, P.; Janssen, D.; Deleuze, M. S. *Phys. Rev. B: Condens. Matter Mater. Phys.* **2003**, *68* (19), 195409.
(32) Forrest, S. R. *Chem. Rev.* **1997**, *97* (6), 1793.
(33) Koma, A. *Surf. Sci.* **1992**, *267* (1−3), 29.
(34) Forrest, S. R.; Burrows, P. E.; Haskal, E. I.; So, F. F. *Phys. Rev. B: Condens. Matter Mater. Phys.* **1994**, *49* (16), 11309.
(35) Ruiz, R.; Nickel, B.; Koch, N.; Feldman, L. C.; Haglund, R. F., Jr.; Kahn, A.; Family, F.; Scoles, G.. *Phys. Rev. Lett.* **2003**, *91* (13), 136102/1.
(36) Meyer Zu Heringdorf, F.-J.; Reuter, M. C.; Tromp, R. M. *Appl. Phys. A: Mater. Sci. Process.* **2004**, *78* (6), 787.
(37) Pratontep, S.; Brinkmann, M.; Nuesch, F.; Zuppiroli, L. *Phys. Rev. B: Condens. Matter Mater. Phys.* **2004**, *69* (16), 165201.
(38) Mayer, A. C.; Ruiz, R.; Headrick, R. L.; Kazimirov, A.; Malliaras, G. G. *Org. Electron.* **2004**, *5* (5), 257.
(39) Lukas, S.; Sohnchen, S.; Witte, G.; Woll, C. *ChemPhysChem* **2004**, *5* (2), 266.
(40) Guaino, P.; Cafolla, A. A.; Carty, D.; Sheerin, G.; Hughes, G. *Surf. Sci.* **2003**, *540* (1), 107.
(41) Image by Chang, K.-C.; Ruiz, R.; Blakely, J.; Malliaras, G. G.; Unpublished.
(42) Zinsmeis, G. *Vacuum* **1966**, *16* (10), 529.
(43) Zinke-Allmang, M.; Feldman, L. C. *Appl. Surf. Sci.* **1991**, *52* (4), 357.
(44) Amar, J. G.; Family, F.; Lam, P.-M. *Phys. Rev. B* **1994**, *50* (12), 8781.
(45) Zinke-Allmang, M.; Feldman, L. C.; Grabow, M. H. *Surf. Sci. Rep.* **1992**, *16* (8), 377.
(46) Blackman, J. A.; Wilding, A. *Europhys. Lett.* **1991**, *16* (1), 115.
(47) Barabási, A.-L.; Stanley, H. E. Submonolayer deposition. In *Fractal Concepts in Surface Growth*; Cambridge University Press: Cambridge, 1995; pp 175−191.
(48) Amar, J. G.; Family, F. *Phys. Rev. Lett.* **1995**, *74* (11), 2066.
(49) Venables, J., *Introduction to Surface and Thin Film Processes*; Cambridge University Press: Cambrige, UK, 2000.
(50) Shtein, M.; Mapel, J.; Benziger, J. B.; Forrest, S. R. *Appl. Phys. Lett.* **2002**, *81* (2), 268.
(51) Yamaguchi, T.× *J. Phys. Soc. Jpn.* **1999**, *68* (4), 1321.
(52) Kasaya, M.; Tabata, H.; Kawai, T.× *Surf. Sci.* **1998**, *400* (1−3), 367.
(53) Chen, Q.; McDowall, A. J.; Richardson, N. V. *Langmuir* **2003**, *19* (24), 10164.
(54) Knipp, D.; Street, R. A.; Volkel, A.; Ho, J. *J. Appl. Phys.* **2003**, *93* (1), 347.
(55) Nichols, J. A.; Gundlach, D. J.; Jackson, T. N. *Appl. Phys. Lett.* **2003**, *83* (12), 2366.
(56) Puntambekar, K. P.; Pesavento, P. V.; Frisbie, C. D. *Appl. Phys. Lett.* **2003**, *83* (26), 5539.
(57) Swiggers, M. L.; Xia, G.; Slinker, J. D.; Gorodetsky, A. A.; Malliaras, G. G. *Appl. Phys. Lett.* **2001**, *79* (9), 1300.
(58) Casalis, L.; Danisman, M. F.; Nickel, B.; Bracco, G.; Toccoli, T.; Iannotta, S.; Scoles, G. *Phys. Rev. Lett.* **2003**, *90* (20), 206101/1.
(59) Nickel, B.; Barabash, R.; Ruiz, R.; Koch, N.; Kahn, A.; Feldman, L. C.; Haglund, R. F., Jr.; Scoles, G. *Phys. Rev. B: Condens. Matter Mater. Phys.* **2004**, *70* (12), 125401.
(60) Schroeder, P. G.; France, C. B.; Park, J. B.; Parkinson, B. A. *J. Appl. Phys.* **2002**, *91* (5), 3010.
(61) Koch, N.; Elschner, A.; Schwartz, J.; Kahn, A.−*Appl. Phys. Lett.* **2003**, *82* (14), 2281.
(62) Schroeder, P. G.; France, C. B.; Park, J. B.; Parkinson, B. A. *J. Phys. Chem. B* **2003**, *107* (10), 2253.
(63) Harada, Y.; Ozaki, H.; Ohno, K. *Phys. Rev. Lett.* **1984**, *52* (25), 2269.
(64) Jentzsch, T.; Juepner, H. J.; Brzezinka, K.-W.; Lau, A. *Thin Solid Films* **1998**, *315* (1−2), 273.
(65) He, R.; Dujovne, I.; Chen, L.; Miao, Q.; Hirjibehedin, C. F.; Pinczuk, A.; Nuckolls, C.; Kloc, C.; Ron, A. *Appl. Phys. Lett.* **2004**, *84* (6), 987.
(66) Northrup, J. E.; Tiago, M. L.; Louie, S. G. *Phys. Rev. B: Condens. Matter Mater. Phys.* **2002**, *66* (12), 121404.
(67) France, C. B.; Schroeder, P. G.; Forsythe, J. C.; Parkinson, B. A. *Langmuir* **2003**, *19* (4), 1274.
(68) Guaino, P.; Carty, D.; Hughes, G.; Moriarty, P.; Cafolla, A. A. *Appl. Surf. Sci.* **2003**, *212−213*, 537.
(69) Schuerlein, T. J.; Schmidt, A.; Lee, P. A.; Nebesny, K. W.; Armstrong, N. R. *Jpn. J. Appl. Phys., Part 1* **1995**, *34* (7B), 3837.
(70) Wang, Y. L.; Ji, W.; Shi, D. X.; Du, S. X.; Seidel, C.; Ma, Y. G.; Gao, H.-J.; Chi, L. F.; Fuchs, H. *Phys. Rev. B: Condens. Matter Mater. Phys.* **2004**, *69* (7), 075408.
(71) Images by Ruiz, R., Unpublished.
(72) Image courtesy of Koch, N., Unpublished.
(73) Lukas, S.; Witte, G.; Woll, C.. *Phys. Rev. Lett.* **2002**, *88* (2), 028301.
(74) Gundlach, D. J.; Lin, Y. Y.; Jackson, T. N.; Nelson, S. F.; Schlom, D. G. *IEEE Electron Device Lett.* **1997**, *18* (3), 87.
(75) Horowitz, G.; Fichou, D.; Peng, X.; Garnier, F. *Synth. Met.* **1991**, *41* (3), 1127.
(76) Knipp, D.; Street, R. A.; Volkel, A. R. *Appl. Phys. Lett.* **2003**, *82* (22), 3907.
(77) Lee, J.; Kim, K.; Kim, J. H.; Im, S.; Jung, D.-Y. *Appl. Phys. Lett.* **2003**, *82* (23), 4169.
(78) Luo, Y.; Wang, G.; Theobald, J. A.; Beton, P. H. *Surf. Sci.* **2003**, *537* (1−3), 241.
(79) Puigdollers, J.; Voz, C.; Orpella, A.; Quidant, R.; Martin, I.; Vetter, M.; Alcubilla, R. *Org. Electron.* **2004**, *5* (1−3), 67.
(80) Dimitrakopoulos, C. D.; Purushothaman, S.; Kymissis, J.; Callegari, A.; Shaw, J. M. *Science* **1999**, *283* (5403), 822.
(81) Dimitrakopoulos, C. D.; Kymissis, I.; Purushothaman, S.; Neumayer, D. A.; Duncombe, P. R.; Laibowitz, R. B. *Adv. Mater.* **1999**, *11* (16), 1372.
(82) Ruiz, R.; Feldman, L. C.; Haglund, R. F., Jr.; McKee, R. A.; Koch, N.; Nickel, B. A.; Pflaum, J.; Scoles, G.; Kahn, A. *Growth and Morphology of Pentacene Films on Oxide Surfaces*. In *Organic Optoelectronic Materials, Processing and Devices*: Symposium, 2002; Materials Research Society: Warrendale, PA, 2003; BB10.54.11−BB10.54.17.
(83) Fritz, S. E.; Martin, S. M.; Frisbie, C. D.; Ward, M. D.; Toney, M. F. *J. Am. Chem. Soc.* **2004**, *126* (13), 4084.
(84) Ruiz, R.; Mayer, A. C.; Malliaras, G. G.; Nickel, B.; Scoles, G.; Kazimirov, A.; Kim, H.; Headrick, R. L.; Islam, Z. *Appl. Phys. Lett.*, accepted for publication.
(85) Wu, J. S.; Spence, J. C. H. *J. Appl. Crystallogr.* **2004**, *37*, 78.
(86) Drummy, L. F.; Miska, P. K.; Martin, D. C. Crystal structure of and defects in the pentacene thin film phase. In *Polymer/Metal Interfaces and Defect Mediated Phenomena in Ordered Polymers: Symposia*; Mater. Res. Soc. Symposium Proceedings Vol. 734); Manias, E., Malliaras, G. G., Eds.; Materials Research Society: Warrendale, PA, 2003; pp 397−401.
(87) Lin, Y.-Y.; Gundlach, D. I.; Nelson, S. F.; Jackson, T. N. *IEEE Trans. Electron Devices* **1997**, *44* (8), 1325.
(88) Gundlach, D. J.; Jia, L. L.; Jackson, T. N. *IEEE Electron Device Lett.* **2001**, *22* (12), 571.
(89) Kobayashi, S.; Nishikawa, T.; Takenobu, T.; Mori, S.; Shimoda, T.; Mitani, T.; Shimotani, H.; Yoshimoto, N.; Ogawa, S.; Iwasa, Y., *Nat. Mater.* **2004**, *3* (5), 317.
(90) Shankar, K.; Jackson, T. N. *J. Mater. Res.* **2004**, *19* (7), 2003.
(91) Weidkamp, K. P.; Hacker, C. A.; Schwartz, M. P.; Cao, X. P.; Tromp, R. M.; Hamers, R. J. *J. Phys. Chem. B* **2003**, *107* (40), 11142.
(92) France, C. B.; Schroeder, P. G.; Parkinson, B. A. *Nano Lett.* **2002**, *2* (7), 693.
(93) Watkins, N. J.; Yan, L.; Gao, Y. L. *Appl. Phys. Lett.* **2002**, *80* (23), 4384.
(94) Zhang, Y. J.; Petta, J. R.; Ambily, S.; Shen, Y. L.; Ralph, D. C.; Malliaras, G. G. *Adv. Mater.* **2003**, *15* (19), 1632.
(95) Zorba, S.; Le, Q. T.; Watkins, N. J.; Yan, L.; Gao, Y. *J. Nanosci. Nanotechnol.* **2001**, *1* (3), 317.
(96) Koch, N.; Ghijsen, J.; Johnson, R. L.; Schwartz, J.; Pireaux, J.-J.; Kahn, A. *J. Phys. Chem. B* **2002**, *106*, 4192.
(97) Koch, N.; Ghijsen, J.; Ruiz, R.; Pflaum, J.; Johnson, R. L.; Pireaux, J.-J.; Schwartz, J.; Kahn, A. *Interaction and energy level alignment at interfaces between pentacene and low work function metals*. In *Organic Optoelectronic Materials, Processing and Devices: Symposium*, 25−30 Nov. 2001, Boston, MA; Materials Research Society: Warrendale, PA, 2002; pp 9−14.
(98) Ozaki, H. *J. Chem. Phys.* **2000**, *113* (15), 6361.
(99) Choudhary, D.; Clancy, P.; Bowler, D. Submitted for publication.
(100) Hughes, G.; Roche, J.; Carty, D.; Cafolla, T.; Smith, K. E. *J. Vacuum Sci. Technol. B* **2002**, *20* (4), 1620.
(101) Choudhary, D.; Clancy, P.; Shetty, R.; Escobedo, F. Submitted for publication.
(102) Dimitrakopoulos, C. D.; Mascaro, D. J. *IBM J. Res. Dev.* **2001**, *45* (1), 11.
(103) Lewis, B. Nucleation and Growth Theory. In *Crystal Growth*, 2nd ed.; Pamplin, B. R.; Pergamon: Oxford, 1980; pp 23−63.
(104) Dodabalapur, A.; Torsi, L.; Katz, H. E. *Science, New Series* **1995**, *268* (5208), 270.
(105) Iannotta, S.; Toccoli, T. *J. Polym. Sci., Part B: Polym. Phys.* **2003**, *41* (21), 2501.
(106) Iannotta, S.; Toccoli, T.; Biasioli, F.; Boschetti, A.; Ferrari, M. *Appl. Phys. Lett.* **2000**, *76* (14), 1845.
(107) Aversa, L.; Verucchi, R.; Ciullo, G.; Ferrari, L.; Moras, P.; Pedio, M.; Pesci, A.; Iannotta, S. *Appl. Surf. Sci.* **2001**, *184* (1−4), 350.
(108) Podesta, A.; Toccoli, T.; Milani, P.; Boschetti, A.; Innotta, S. *Surf. Sci.* **2000**, *464* (1), L673.
(109) Milani, P.; Iannotta, S. *Cluster Beam Synthesis of Nanostructured Materials*; Springer-Verlag: Berlin, 1999.
(110) Iannotta, S.; Toccoli, T.; Ferrari, M.; Ronchin, S.; Podesta, A.; Milani, P.; Scardi, P. *Proc. SPIE−Int. Soc. Opt. Eng.* **2000**, *3939*, 135.
(111) Umbach, E.; Glockler, K.; Sokolowski, M. *Surf. Sci.* **1998**, *402−404*, 20.
(112) Witten, T. A., Jr.; Sander, L. M. *Phys. Rev. Lett.* **1981**, *47* (19), 1400.
(113) Warren, B. E. *X-ray Diffraction*; Addison-Wesley: Reading, MA, 1969.

(114) Vlieg, E.; Denier van der Gon, A. W.; van der Veen, J. F.; Macdonald, J. E.; Norris, C. *Phys. Rev. Lett.* **1988**, *61* (19), 2241.
(115) Fenter, P.; Eisenberger, P.; Burrows, P.; Forrest, S. R.; Liang, K. S. *Physica B* **1996**, *221* (1−4), 145.
(116) Krause, B.; Schreiber, F.; Dosch, H.; Pimpinelli, A.; Seeck, O. H. *Europhys. Lett.* **2004**, *65* (3), 372.
(117) Cohen, P. I.; Petrich, G. S.; Pukite, P. R.; Whaley, G. J.; Arrott, A. S. *Surf. Sci.* **1989**, *216* (1−2), 222.
(118) Schwoebel, R. L.; Shipsey, E. J. *J. Appl. Phys.* **1966**, *37* (10), 3682.
(119) Weschke, E.; Schussler-Langeheine, C.; Meier, R.; Kaindl, G.; Sutter, C.; Abernathy, D.; Grubel, G. *Phys. Rev. Lett.* **1997**, *79* (20), 3954.
(120) Burton, W. K.; Cabrera, N.; Frank, F. C. *Philos. Trans. R. Soc. London, Ser. A* **1951**, *243* (866), 299.

CM049563Q